Direct Comparison of the Solution Structure of a C_1-Symmetric Pinane-Fused Cyclopentadienyllithium with the Stereoselectivity of Its Capture by Electrophiles[1]

Walter Bauer,*[,†] Mark R. Sivik,[‡,2] Dirk Friedrich,[‡] Paul von Ragué Schleyer,[†] and Leo A. Paquette*[,‡]

Institut für Organische Chemie der Universität Erlangen-Nürnberg, Henkestrasse 42, D-8520 Erlangen, Federal Republic of Germany, and Evans Chemical Laboratories, The Ohio State University, Columbus, Ohio 43210

Received July 15, 1992

The verbenone-derived cyclopentadienyl compound (1*S*,8*S*)-7,7,9,9-tetramethyltricyclo[6.1.1.0^{2,6}]deca-2,5-dienyllithium (VCpLi) yielded a 3:2 mixture of exo and endo deuterio quench products upon reaction with D_2O at −78 °C in THF. Stereochemical identification was achieved by NMR analysis of Diels–Alder addition products. Reaction of VCpLi with Me_3SiCl under the same conditions gave rise to a 9:1 exo:endo product mixture. Silatropic shifts were observed in these quench products. According to NMR analysis, VCpLi consists nearly exclusively of the *exo*-Li monomer in THF at +26 °C. However, at −80 °C a ternary equilibrium of an *exo*-Li monomer, an *exo,exo*-Li sandwich dimer, and an *endo,endo*-Li sandwich dimer in a 5.1:2.8:1.0 molar ratio has been detected. Thermodynamic parameters for the monomer-dimer equilibrium are $\Delta H° = -3.6 \pm 0.2$ kcal/mol and $\Delta S° = -15.6 \pm 0.9$ eu. Due to ring current effects, unusual upfield ^{6}Li chemical shifts are observed: δ (ppm) = −7.83 (exo monomer), −12.22 (exo,exo dimer), and −12.25 (endo,endo dimer). Exo/endo assignment of the isomers of VCpLi was achieved by ^{6}Li, ^{1}H HOESY. MNDO calculations correctly reflect the relative stabilities of the individual isomers of VCpLi as well as the temperature dependence of the monomer–dimer equilibrium.

Lithium cations can interact with cyclopentadienide rings in rather intricate ways. For CpLi and its simple substituted derivatives, the lithium atom is centrally η^5 bound to the Cp^- ring at room temperature.[3] NMR spectral analyses of CpLi solutions in THF-d_8 below −100 °C reveal a monomer–dimer equilibrium.[4] Since the coalescence temperature of this dynamic exchange is quite low, the associated rates are necessarily very fast.

These processes are slowed considerably when the Cp ring is grafted to nonplanar frameworks, e.g., based on norbornane[4] or bornane.[5] Furthermore, these species exhibit π-facial stereoselectivity not present in simpler systems. For example, lithium isodicyclopentadiene (IsodiCpLi) exists at low temperatures as an equilibrium mixture of the exo contact ion pair monomer **1** and dimer **2** having one lithium sandwiched between the exo faces

1

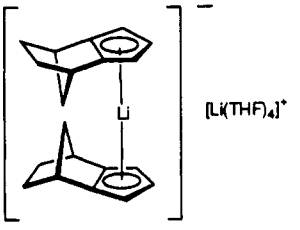

2

of the two anion moieties. Under comparable conditions, the camphor analogue (CCpLi) exists as a three-component aggregate consisting of the *endo*- and *exo*-lithio monomers and the *endo,endo*-lithio dimer. These strikingly different complexation stereoselectivities impact on the course of their stereochemically divergent chemical reactions.[6]

These considerations have prompted us to examine the dynamic states, aggregation profiles, and stereochemical facets of lithium coordination to a highly optically enriched pinane-fused congener. The preparation of (+)-**3** from (1*S*,5*S*)-(−)-verbenone was reported several years ago.[7] Its conversion to transition metal complexes typified by **4** and **5** (M = Ti and Zr)[7,8] with significant face discrimination

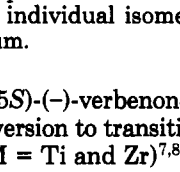

3

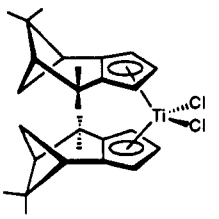

4

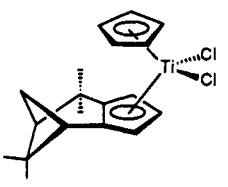

5

was rationalized on the basis of a steric bias against endo coordination. To understand the role of Li^+ in directing this stereochemical outcome, (−)-**6** has now been metalated

† Institut für Organische Chemie.
‡ Evans Chemical Laboratories.

(1) Isodicyclopentadienes and Related Molecules. 59. Part 58: Reference 5.
(2) National Need Fellow, 1989, 1990; Amoco Foundation Fellow, 1991.
(3) Jutzi, P. *Adv. Organomet. Chem.* **1986**, *26*, 217.
(4) Paquette, L. A.; Bauer, W.; Sivik, M. R.; Bühl, M.; Feigel, M.; Schleyer, P. v. R. *J. Am. Chem. Soc.* **1990**, *112*, 8776. See also: Eiermann, M.; Hafner, K. *J. Am. Chem. Soc.* **1992**, *114*, 135.
(5) Bauer, W.; O'Doherty, G. A.; Schleyer, P. v. R.; Paquette, L. A. *J. Am. Chem. Soc.* **1991**, *113*, 7093.
(6) (a) Paquette, L. A.; Charumilind, P. *J. Am. Chem. Soc.* **1982**, *104*, 3749. (b) Paquette, L. A.; Charumilind, P.; Kravetz, T. M.; Böhm, M. C.; Gleiter, R. *J. Am. Chem. Soc.* **1983**, *105*, 3126. (c) Paquette, L. A.; Charumilind, P.; Gallucci, J. C. *J. Am. Chem. Soc.* **1983**, *105*, 7364. (d) Paquette, L. A.; Hayes, P. C.; Charumilind, P.; Böhm, M. C.; Gleiter, R.; Blount, J. F. *J. Am. Chem. Soc.* **1983**, *105*, 3136. (e) Paquette, L. A.; McKinney, J. A.; McLaughlin, M. L.; Rheingold, A. L. *Tetrahedron Lett.* **1986**, 5599. (f) Paquette, L. A.; Moriarty, K. J.; McKinney, J. A.; Rogers, R. D. *Organometallics* **1989**, *8*, 1707.
(7) Moriarty, K. J.; Rogers, R. D.; Paquette, L. A. *Organometallics* **1989**, *8*, 1512.
(8) Sivik, M. R.; Rogers, R. D.; Paquette, L. A. *J. Organomet. Chem.* **1990**, *397*, 177.

0276-7333/92/2311-4178$03.00/0

with the ^6Li isotope for characterization of the anion by NMR. The levorotatory antipode was used, as it can be obtained in high optical purity (99% ee).[9] In addition, the stereoselectivity of product distributions resulting from condensation with more conventional electrophiles has been assessed. The strikingly distinctive nature of the lithium salt of **6** provides added insight into the interrelationship of lithium cyclopentadienide structure and product stereochemistry.

Results

Electrophilic Capture Experiments. The lithium salt of **6** was dissolved in dry tetrahydrofuran and added at −78 °C to an excess of D_2O in the same solvent. The two products obtained in a 60:40 ratio were identified as **7** and **8** on the basis of ^2H NMR analysis and their conversion into **9** and **10**, respectively. Previously, it had been noted

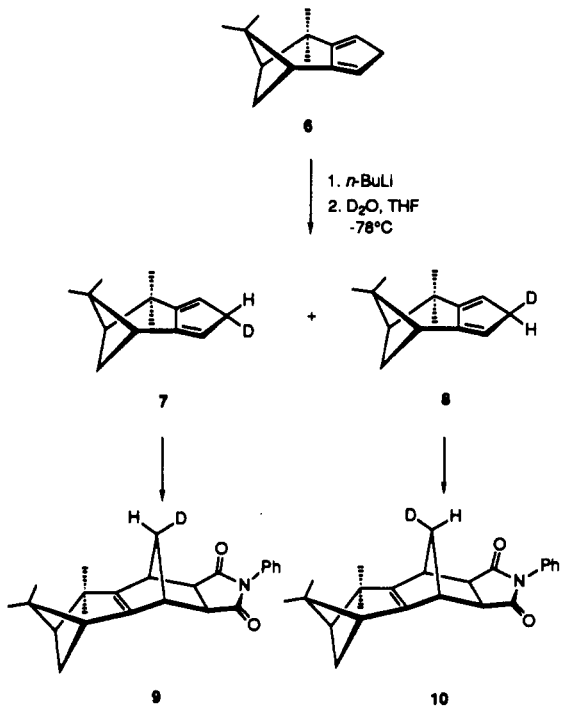

that the geminal methylene protons of the Cp ring in **6** are almost coincident in C_6D_6 solution. However, in acetone-d_6 these protons become sufficiently distinguished to allow the product ratio to be determined by integration of the corresponding ^2H resonances (δ 2.91 and 2.82, respectively). The ^{13}C NMR spectrum of the **7**/**8** mixture is a superposition of two unresolved sets of signals stemming from the epimeric pair of d_1-hydrocarbons. Significantly, however, the exclusive appearance of a *C*HD resonance for the C4 center (δ 40.48, 1:1:1 triplet, $J_{C,D}$ = 19.2 Hz) is direct evidence that the level of deuterium incorporation approaches 100%, as also is seen from integration of the proton spectrum.

Further evidence that the observed stereoselectivity is genuinely intrinsic to this chiral cyclopentadiene was gained by deprotonation of the **7**/**8** mixture followed by a water quench at −78 °C. The composition of the resulting d_1 molecules was reversed (45% of **7**, 55% of **8**).

Dienes **7** and **8** undergo efficient Diels–Alder condensation with *N*-phenylmaleimide in benzene solution at room temperature. The **9**/**10** product mixture is characterized by a well-resolved ^1H NMR spectrum in $CDCl_3$. This is particularly true of each of the methylene protons geminal to the deuterium label. In **9**, this proton is situated above the central double bond and is deshielded (δ 1.31). Integration of these resonances showed the product distribution to be 58:42, closely matching the value determined earlier.

The assignment of relative stereochemistry to **9** and **10** by NOE experiments was complicated initially since two of the methyl groups are not well resolved in $CDCl_3$ solution. However, since all four CH_3 signals are conveniently separated in C_6D_6, the combined results of NOE data garnered from both spectra allowed the complete identification of all ^1H resonances. A single *C*HD resonance appeared for the apical norbornenyl carbons, due to the high-d_1 content.

Exposure of cold (−78 °C) THF solutions of the lithium salt of **6** to chlorotrimethylsilane afforded the isomeric silanes **11** and **12** as a 9:1 mixture. The major constituent, obtained pure in 83% yield by HPLC (recycle mode), exhibited the stereochemically definitive NOE enhancement illustrated in **11**. As is customary for such silanes,[6c] [1,5] silatropic migration within **11** was competitive with the formation of Diels–Alder adducts in the 20–25 °C temperature range. In the condensation involving *N*-phenylmaleimide, conversion to a 5:1 mixture of **14** and **15** was observed. Although complete chromatographic

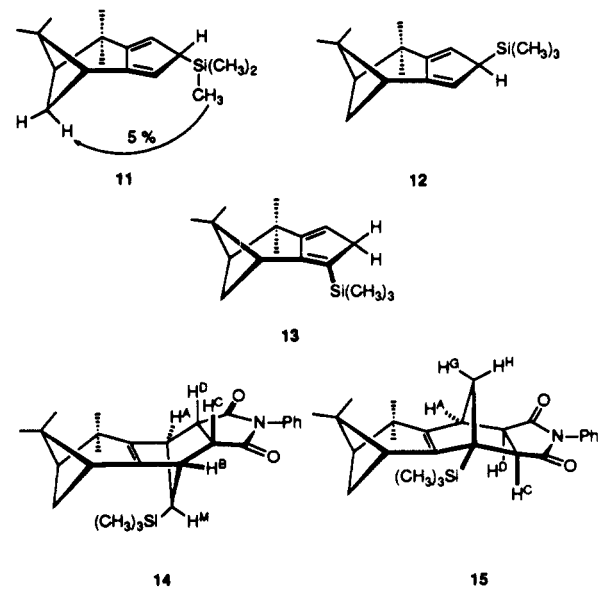

separation could not be accomplished, it proved possible to enrich the level of **15** sufficiently so that definitive decoupling experiments could be performed on equimolar concentrations of the two isomers. By this means, it proved possible to assign all proton resonances to both compounds. The relative stereochemistry within the norbornene components of **14** and **15** could be deduced by the presence or absence of diagnostic long-range couplings. Thus, the very small $^3J_{A,D}$ and $^3J_{B,C}$ spin interactions in the spectrum of **14** require exo orientation of the maleimide ring. Further, the absence of the W couplings $^4J_{C,M}$ and $^4J_{D,M}$ is consistent only with syn orientation of H^M and the imide unit. While $^3J_{A,D}$ in **15** is again close to zero, the W couplings $^4J_{D,G}$ and $^4J_{C,G}$ (both 1.5 Hz) are clearly evident. Beyond this, the assignment of structure **15** is based on capture from the less sterically congested face anti to the gem-dimethyl bridge of **13** since guidance by the Me_3Si group is now lacking.

While the methylation of the lithium salt of **6** with methyl iodide afforded an inseparable mixture of several compounds, a major adduct could be isolated after cyclo-

(9) Sivik, M. R.; Paquette, L. A. *Org. Synth.*, submitted for publication.

addition with *N*-phenylmaleimide. The protons of its imide ring exhibit no coupling to adjacent bridgehead protons. Further, the appearance of a single olefinic resonance and of five methyl singlets, as well as the presence in the ^{13}C NMR spectrum of four quaternary, four methine, and two methylene carbons are indicative that while methylation did occur at the central Cp carbon, [1,5] prototropic shift ensued to give either **16** or **17** prior to the

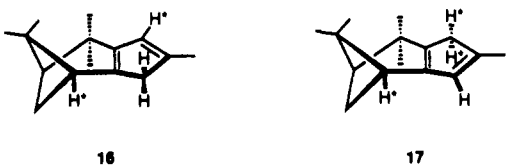

16 **17**

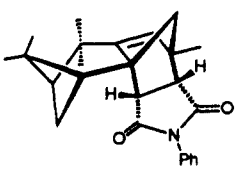

18

Diels–Alder reaction. While the asterisked hydrogen atoms in **16** are nicely staggered relative to the proximal "peri" substituents, **17** is eclipsed. Torsional effects should therefore favor conversion to **16**. For these reasons, as well as the absence of W couplings involving the anti proton of the apical methylene bridge, the compound was formulated as endo adduct **18**. This assignment was subsequently verified by NOE studies on C_6D_6 solutions since in this solvent (but not $CDCl_3$) the ^1H NMR spectrum is particularly well resolved.

To circumvent this isomerization, the lithium salt of **6** was treated with 1-bromo-2-chloroethane-2,2-d_2[6b,10] in order to generate isotopically labeled spirocyclopropylidenes **19** and **20**. As the first alkylation is independent of the

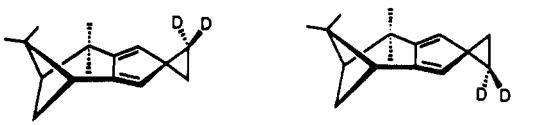

19 **20**

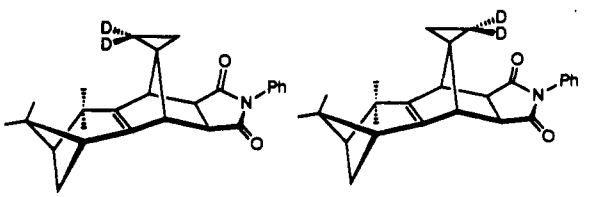

21 **22**

second, the latter is solely responsible for defining the face of cyclopentadienide capture. Determination of the diastereomeric ratio of **19** and **20** was frustrated by the mutual overlap of the cyclopropyl protons (in ^1H NMR), deuterons (in ^2H NMR), and carbons (in ^{13}C NMR) in a variety of solvents. Consequently, recourse was again made to the *N*-phenylmaleimide adducts,[11] where the individual CH_2CD_2 AB multiplets were well separated. These appeared at 0.56 and 0.40 ppm in $CDCl_3$ solution (relative intensity ratio = 58:42). Double irradiation of the syn apical methyl signal immediately showed that **22** was more prevalent than **21** and therefore that **20** was the kinetically favored spiroalkylation product.

(10) (a) Francis, J. E.; Leitch, L. C. *Can. J. Chem.* **1957**, *35*, 502. (b) Kovachic, D.; Leitch, L. C. *Can. J. Chem.* **1961**, *39*, 363.

(11) The usual assumption inherent in such experiments that product distributions are not altered because of differential reactivity applies here as well.

NMR Investigations of 23, the Lithium Salt of 6, at Room Temperature

^1H and ^{13}C NMR Spectra. For the NMR investigations of the lithium salt of **6**, material enriched 96% with the ^6Li isotope[12] was employed. For convenience, the numbering and stereochemical assignments shown in **23** were utilized herein.

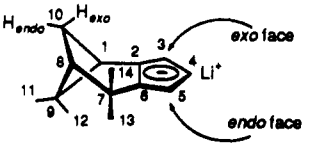

23

The ^1H and ^{13}C NMR spectra of **23** in THF-d_8 at 26 °C both consist of a single set of signals (Tables I and II), indicative either of the existence of one species or of rapid exchange between different aggregates. Proper assignments to these spectra were achieved by a combination of two-dimensional NMR methods (COSY, ^1H, ^{13}C HETCOR, COLOC[13a] that are not discussed herein). As will be demonstrated, **23** consists nearly exclusively of exo monomer **24** in THF at 26 °C. Hydrogen atoms H1 and H8 show appreciable W-type coupling ($^4J_{H1,H8}$ = 5.6 Hz), consistent with data for bicyclo[1.1.1]pentane ($^4J_{H1,H3}$ = 18 Hz).[14] One of the geminal protons shows no vicinal coupling to H1 or to H8. As is evident from inspection of a molecular model, H10(exo) must be involved. Both dihedral angles H10(exo)/H1 and H10(exo)/H8 are each close to 90° (Karplus relationship).[13b-d]

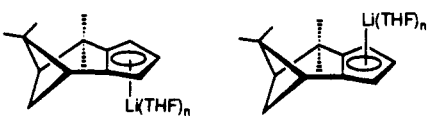

24 **25**

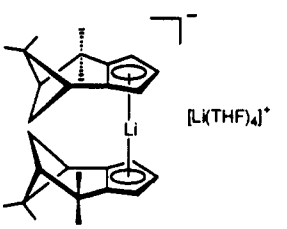

26

A ROESY spectrum[13a] recorded on the same solution at 26 °C allowed further assignment of the ^1H NMR signals of **23**. Figure 1 illustrates a series of f_1 cross sections from the ROESY matrix. Significantly, diagonal signals are directed downward whereas ROE cross peaks appear as upward signals. HOHAHA cross peaks due to coherence transfer from scalar coupling appear as antiphase signals.[15] Slices 2–4 involve the chemical shifts of the Cp protons H3, H4, and H5. In slice, 4, a bridgehead proton cross peak

(12) (a) Seebach, D.; Hässig, R.; Gabriel, J. *Helv. Chim. Acta* **1983**, *66*, 308. (b) Fraenkel, G.; Hsu, H.; Su, B. M. In Bach, R. O., Ed.; *Lithium. Current Applications in Science, Medicine, and Technology*; Wiley: New York, 1985. (c) Günther, H.; Moskau, D.; Bast, P.; Schmalz, D. *Angew. Chem.* **1987**, *99*, 1242. *Angew. Chem., Int. Ed. Engl.* **1987**, *26*, 1212.

(13) (a) Kessler, H.; Gehrke, M.; Griesinger, C. *Angew. Chem.* **1988**, *100*, 507. *Angew. Chem., Int. Ed. Engl.*, **1988**, *27*, 490. (b) Karplus, M. *J. Chem. Phys.* **1959**, *30*, 11. (c) Karplus, M. *J. Chem. Phys.* **1960**, *33*, 1842. (d) Karplus, M. *J. Am. Chem. Soc.* **1963**, *85*, 2870.

(14) Padwa, A.; Shefter, E.; Alexander, E. *J. Am. Chem. Soc.*, **1968**, *90*, 3717.

(15) Neuhaus, D.; Williamson, M. *The Nuclear Overhauser Effect in Structural and Conformational Analysis*; VCH: New York, 1989.

Table I. ^{1}H NMR Chemical Shifts of 23, 24, 26, and 27 (δ (ppm), 0.35 M, THF-d_8) at 26 and at −90 °C[a,b] (For Numbering, See Formula 23)

H	23 (26 °C)	24 (−90 °C)	26 (−90 °C)	27 (−90 °C)
1	2.44 (dd, 5.6; 5.6 Hz)	2.45 (dd, 5.3; 5.3 Hz)	2.29 (dd, 5.3; 5.3 Hz)	2.29 (dd, 5.3; 5.3 Hz)
3	5.22 (dd, 2.6; 2.6 Hz)	5.24 (nr)	4.86 (nr)	4.88 (nr)
4	5.43 (dd, 2.6; 2.6 Hz)	5.45 (nr)	4.97 (dd, 3.1; 3.1 Hz)	4.95 (nr)
5	5.30 (dd, 2.6; 2.6 Hz)	5.29 (dd, 2.8; 2.8 Hz)	5.10 (nr)	5.10 (nr)
8	1.69 (dd, 5.6; 5.6 Hz)	1.69 (dd, 5.6; 5.6 Hz)	1.55 (dd, 5.6; 5.6 Hz)	1.55 (dd, 5.6; 5.6 Hz)
10 (endo)	2.50 (ddd, 8.5; 5.6; 5.6 Hz)	2.51 (ddd, 8.2; 5.5; 5.5 Hz)	2.35 (m)	2.35 (m)
10 (exo)	1.58 (d, 8.5 Hz)	1.50 (d, 8.2 Hz)	1.92 (d, 8.2 Hz)	1.92 (d, 8.2 Hz)
11	1.31 (s)	1.32 (s)	1.26 (s)	1.22 (s)
12	0.52 (s)	0.56 (s)	0.42 (s)	1.06[c] (s)
13	1.18 (s)	1.18 (s)	1.04 (s)	1.18 (s)
14	1.18 (s)	1.16 (s)	1.22 (s)	1.22 (s)

[a] The chemical shifts of the carbons and protons at positions 3, 4, and 5 in **26** and **27** could not be assigned unambiguously even by C,H HETCOR and COLOC spectra. The assignment given is based on the assumption that of C3, C4, and C5 in both **26** and **27**, C4 has the largest chemical shift. Likewise, in both **26** and **27**, H3 is assumed to appear at higher field than both H4 and H5. [b] Abbreviations: s (singlet), d (doublet), m (multiplet), nr (not resolved). [c] We noted a discrepancy in the assignment of H12 in **27** based on the results of Figure 3 vs the results of Figure 4. The value given in this table is derived from Figure 4. According to Figure 3, δ_{H12} (**27**) would be 0.80 ppm.

Table II. ^{13}C Chemical Shifts of 23, 24, 26, and 27 (δ (ppm), THF-d_8, 0.35 M) at 26 and at −90 °C[a] (For Numbering, See Formula 23 in the Text)

C	23 (26 °C)	24 (−90 °C)	26 (−90 °C)	27 (−90 °C)
1	45.39	44.68	44.48	44.48
2	124.53	123.91	122.52	122.39
3	98.67	98.29	98.56	98.49
4	98.53	98.37	99.03	99.23
5	97.99	97.41	98.20	98.03
6	121.20	120.30	118.60	118.60
7	38.20	38.06	38.30	38.30
8	57.32	56.00	56.37	56.35
9	46.06	45.79	45.60	45.60
10	35.04	34.98	34.02	34.00
11	29.00	28.74	28.95	28.95
12	25.95	26.05	26.05	26.05
13	29.76	29.57	30.23	30.20
14	34.31	34.46	33.34	33.19

[a] See footnote *a* in Table I.

is observed. Thus, the diagonal and the cross-peak signals must be due to H3 and H1, respectively. The complementary cross-peak appears at the chemical shift of H3 in 6. In addition, 6 reveals an antiphase cross peak to H8 due to the scalar H1/H8 coupling. Additional ROE cross-peaks in the same slice involve H10(exo) and the methyl protons H11 and H12. Consistent with distances deduced from a molecular model, the cross-peak involving H1 and methyl protons H11 is more intense than the analogous one that relates H1 to H12. As a consequence

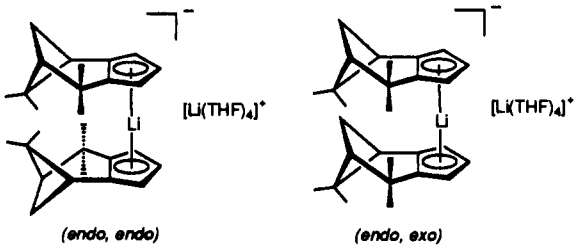

(endo, endo) **27** (endo, exo) **28**

of the unambiguous assignment to H11 and H12 from slice 6, the remaining singlet of methyl protons at δ = 1.18 must be due to the accidentally isochronous signals of H13 and H14. This conclusion was confirmed by inspection of slice 7 where an intense cross-peak was found between bridgehead proton H8 and the spatially proximate methyl groups H13 and H14.

No unambiguous assignment could be deduced for H4 and H5: slices 2 (assigned to H4) and 3 (assigned to H5) both exhibit a weak cross-peak to H13/H14. In CCpLi (**29**)

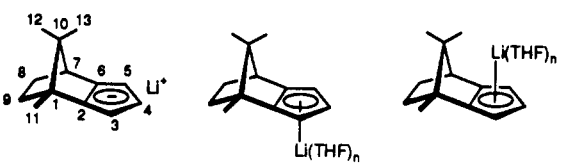

29 **30** **31**

the chemical shift of central Cp carbon atom C4 in endo monomer **30** is larger than the chemical shift of C5. By analogy (obtained from a C,H HETCOR experiment), we conclude that the ^{1}H NMR signal at lowest field in Figure 1 is due to H4 of **23**, in agreement with the assignments reported for titanium complex **32**.[8] Unfortunately, no cross peaks pertinent to the conclusive assignment of H4 and H5 were observed in a ^{1}H, ^{13}C COLOC spectrum of **23**.

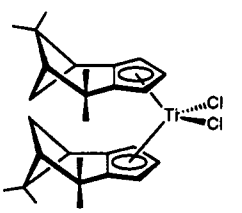

32

Identification of methyl protons H11 (δ 1.31) in Figure 1 was corroborated by inspection of slice 5, where H10(endo) clearly exhibits the only cross-peak to the three methyl singlets in the spectrum. The complementary slice 9 (H11) shows cross-peaks to H10(endo), H1, H8, and H12.

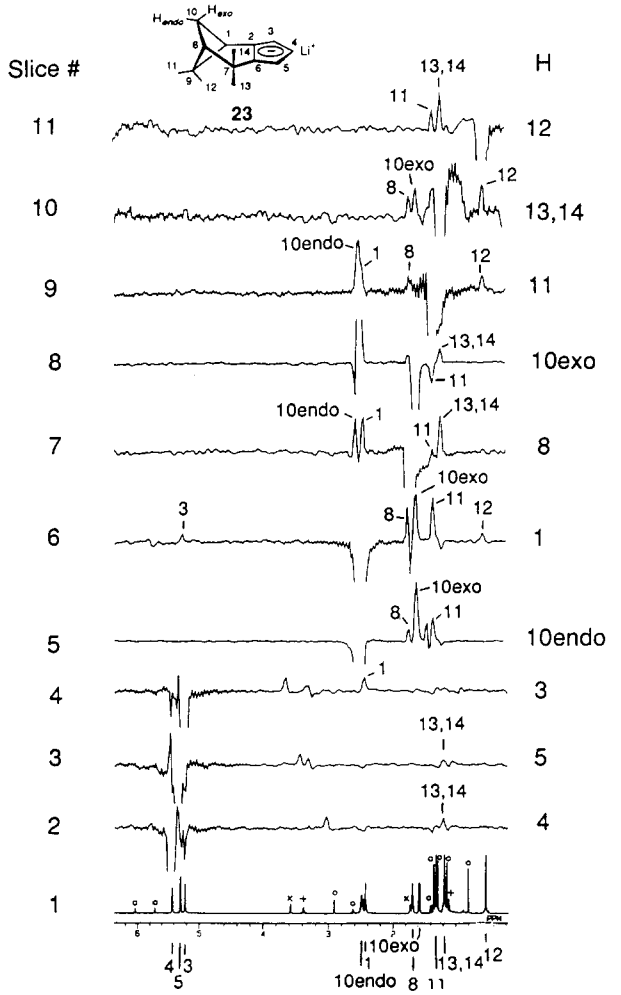

Figure 1. Phase-sensitive ROESY spectrum of **23** (26 °C, 0.35 M, THF-d_8). Only f_1 cross sections cut at the indicated ^{1}H chemical shifts are shown. For numbering, see formula **23**. Slice 1 is a high-resolution one-dimensional spectrum. Diagonal peaks and ROE cross peaks appear as downward and upward signals, respectively. Symbols in slice 1 are × = solvent, + = diethyl ether, ○ = educt **6**. Numbers within slices 2–11 assign cross peaks which involve the indicated H positions.

Slice 8 (H10(exo)) shows an expected ROE to methyl group H14. Interestingly, the same slice reveals a *negative* ROE to methyl protons H11, attributable to an indirect effect propagated by H10(endo).[15]

The chemical shift of the H12 protons is very small (δ = 0.52), consistent with the location of these protons in the "shielding" cone of the aromatic Cp ring. This is in agreement with earlier observations made for CCpLi (**29**).[5] Thus, when the lithium is positioned endo as in **30**, the methyl protons H13 resonate at δ = 0.14. On the other hand, exo orientation of the lithium as in **31** partly cancels this high-field shift (δ_{H13} = 0.85). Since in **23** the shielding effect of the Cp ring on the H12 protons is diminished due to the structurally inherent distance factor, lithium can be confidently assumed to be located predominantly on the exo face of **23** under these conditions. This conclusion will be confirmed by other observations to be described below.

In the ^{13}C NMR spectrum of **23**, the four quaternary carbon atoms C2, C6, C7, and C9 were assigned on the basis of a COLOC[13a] spectrum (not shown here). The signal at δ = 124.53 shows a cross-peak to H10(endo) and H10(exo) resulting from ^3J coupling and must therefore be due to C2. For the alternative C6 signal, a ^4J coupling should be involved and these types of cross peaks are not

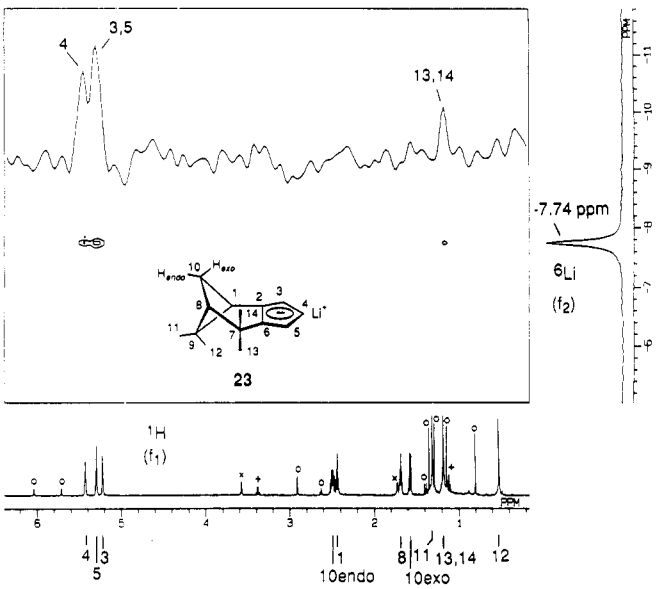

Figure 2. Phase-sensitive ^{6}Li,^{1}H HOESY contour plot of **23** (THF-d_8, 0.35 M, 26 °C), mixing time 2.0 s. The inset shows the f_1 cross section cut at the chemical shift of the ^{6}Li signal. Symbols in the one-dimensional ^{1}H spectrum are as those of Figure 1.

usually observed in COLOC spectra. By analogy, the signal at δ = 121.20 (C6) has a cross-peak to H8 due to ^3J coupling. Identification of the signal at δ = 46.06 as C9 stems from a cross peak to H12 (^2J coupling). For the same reasons, the signal at δ = 38.20, which shows a cross peak to H13/14, must be attributed to C7.

^{6}Li NMR Spectra. The one-dimensional ^{6}Li spectrum of **23** consists of a single resonance at δ = −7.74 ppm in THF-d_8 at 26 °C (Figure 2). This unusual high-field shift may be explained by ring current effects since contact ion pairing (CIP) in **24** positions the lithium in the shielding cone of the aromatic Cp ring. Similar observations have been made for cyclopentadienyllithium,[4] for IsodiCpLi (**1**),[4] and for CCpLi (**29**).[5]

Short Li,H internuclear distances may be detected by using ^{6}Li,^{1}H heteronuclear Overhauser effect spectroscopy (HOESY). We[16] and others[17] have applied this method

(16) (a) Bauer, W.; Schleyer, P. v. R. *J. Am. Chem. Soc.*, **1989**, *111*, 7191. (b) Bauer, W.; Feigel, M.; Müller, G.; Schleyer, P. v. R. *J. Am. Chem. Soc.* **1988**, *110*, 6033. (c) Bauer, W.; Winchester, W. R.; Schleyer, P. v. R. *Organometallics* **1987**, *6*, 2371. (d) Bauer, W.; Clark, T.; Schleyer, P. v. R. *J. Am. Chem. Soc.* **1987**, *109*, 970. (e) Bauer, W.; Müller, G.; Pi, R.; Schleyer, P. v. R. *Angew. Chem.* **1986**, *98*, 1130. *Angew. Chem., Int. Ed. Engl.* **1986**, *25*, 1103. (f) Bauer, W.; Klusener, P. A. A.; Harder, S.; Kanters, J. A.; Duisenberg, A. J. M.; Brandsma, L.; Schleyer, P. v. R. *Organometallics* **1988**, *7*, 552. (g) Gregory, K.; Bremer, M.; Bauer, W.; Schleyer, P. v. R.; Lorenzen, N. P.; Kopf, J.; Weiss, E. *Organometallics* **1990**, *9*, 1485. (h) Hoffmann, D.; Bauer, W.; Schleyer, P. v. R. *J. Chem. Soc., Chem. Commun.* **1990**, 208. (i) Bauer, W.; Schleyer, P. v. R. In Snieckus, V., Ed.; *Advances in Carbanion Chemistry*; Jai, Press: Greenwich, CT, in press. (j) Bauer, W.; Schleyer, P. v. R. *Magn. Reson. Chem.*, **1988**, *26*, 827. (k) Anders, E.; Opitz, A.; Bauer, W. *Synthesis* **1991**, 1221. (l) Edelmann, F. T.; Knösel, F.; Pauer, F.; Stalke, D.; Bauer, W. *J. Organomet. Chem.* **1992**, *438*, 1. (m) Bauer, W.; Hampel, F. *J. Chem. Soc., Chem. Commun.* **1992**, 903.

(17) (a) Günther, H. *Proceedings of the 10th National Conference on Molecular Spectroscopy with International Participation*; Bulgarian Academy of Science: Blagdoevgrad, Bulgaria, 1988. (b) Harder, S.; Boersma, J.; Brandsma, L.; van Mier, G. P. M.; Kanters, J. A. *J. Organomet. Chem.*, **1989**, *364*, 1. (c) Moene, W.; Vos, M.; de Kanter, F. J. J.; Klumpp, G. W.; Spek, A. L. *J. Am. Chem. Soc.* **1989**, *111*, 3463. (d) Arnett, E. M.; Fisher, F. J.; Nichols, M. A.; Ribeiro, A. A. *J. Am. Chem. Soc.* **1989**, *111*, 748. (e) Arnett, E. M.; Fisher, F. J.; Nichols, M. A.; Ribeiro, A. A. *J. Am. Chem. Soc.* **1990**, *112*, 801. (f) Harder, S.; Boersma, J.; Brandsma, L.; Kanters, J. A.; Duisenberg, A. J. M.; van Lenthe, J. H. *Organometallics* **1990**, *9*, 511. (g) Nichols, M. A.; McPhail, A. T.; Arnett, E. M. *J. Am. Chem. Soc.* **1991**, *113*, 6222. (h) Sethson, I.; Johnels, D.; Lejon, T.; Edlund, U.; Wind, B.; Sygula, A.; Rabideau, P. W. *J. Am. Chem. Soc.* **1992**, *114*, 953. (i) Balzer, H.; Berger, S. *Chem. Ber.* **1992**, *125*, 733.

to an increasing number of organolithium compounds. In Figure 2 where the ^{6}Li,^{1}H HOESY contour plot of **23** is seen along with the pertinent f_1 cross section, intense cross peaks involving the ^{1}H chemical shifts of its Cp protons are readily detected. Tight location of lithium above the Cp ring is responsible for this phenomenon as required by a CIP.[18] Differentiation between the placement of lithium on the exo or the endo face of **23** should in principle be possible by ^{6}Li,^{1}H HOESY:endo lithium would produce cross-peaks at both H12 and H13, whereas exo lithium would give rise to a single cross peak at H14. Unfortunately in this special instance, the resonances of methyl protons H13 and H14 are accidentally isochronous at 26 °C. Consequently, the observed single high-field cross peak in Figure 2 could be due to both H13 and H14. However, the lack of a cross peak at the chemical shift of H12 provides indirect evidence that the lithium cation is located (at least predominantly) on the exo face of **23** near room temperature in THF-d_8.

NMR Investigations of 23 at Low Temperatures

^{1}H and ^{13}C NMR Spectra. At −80 °C and below, the ^{1}H and ^{13}C NMR spectra of a 0.35 M solution of **23** in THF-d_8 both show *three* sets of signals (see Tables I and II). The observed species could be the monomers **24** or **25**, as well as the dimers **26**, **27**, or **28**. Since the signal sets are present in different integration ratios, exo,endo dimer **28** can be ruled out because this isomer should exhibit two signal sets in an integral ratio of 1:1. Hence, a *ternary* equilibrium is evidently established under these conditions. To our knowledge, this is only the second reported example of an observed ternary equilibrium in THF. We described the first example for CCpLi (**29**).[5] Note, however, that the change from bornyl fusion to pinane fusion has not impacted negatively on this coordinative preference.

Figure 3 shows the C,H HETCOR spectrum of **23** in THF-d_8 at −90 °C. In the one-dimensional ^{1}H NMR spectrum of **23**, one set of the Cp ring protons resonates appreciably downfield from the remaining two. The low-field set is assigned to a monomer and each of the two high-field sets to a sandwich dimer in agreement with the observations made for the monomeric and dimeric IsodiCpLi's **1** and **2**,[4] as well as for the CCpLi isomers **30**, **31**, and **33**.[5]

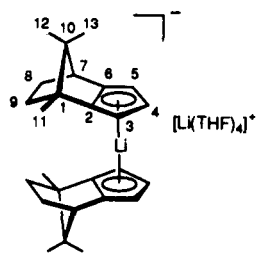

33

Although **28** can be ruled out from the non-even signal intensities, dimers **26** and **27** seem to be present. Since the ^{1}H and ^{13}C NMR chemical shifts of the observed monomer are nearly identical with those observed at room temperature, the species must have exo-complexed lithium as in **24**.

The proportion of monomer to dimers is strongly dependent on the temperature (see below, Thermodynamics section). By contrast, the ratio of the two dimers is constant over the temperature range of −80 to −110 °C (major:minor isomer = 2.8). At temperatures above ca. −70 °C, coalescence of the monomer and dimer signals was observed in both the ^{1}H and the ^{13}C NMR spectra. The ^{1}H NMR signal set of the major dimer shows a methyl proton resonance at quite high field (δ = 0.42). Similar observations were made for protons H13 in the CCpLi sandwich dimer **33**.[5] For comparison, the chemical shift of H13 in **30** is lower by 0.2 ppm. Hence, we assign the upfield ^{1}H NMR peaks at δ = 0.42 in Figure 3 to the syn methyl protons H12 in dimer **26**. A ternary equilibrium of exo monomer **24**, exo,exo dimer **26** and endo,endo dimer **27** is therefore being observed in THF-d_8 at low temperatures. The endo monomer **25** and the mixed exo,endo dimer **28** obviously are not present in detectable amounts under these conditions. As in **24**, the strong upfield shift of the H12 protons in **26** must be a consequence of a magnetic anisotropic environment resulting from their projection into the shielding cone of the adjacent Cp ring. By comparison to **31**, the shielding effect in **27** is compensated for by the presence of a spatially close lithium cation.[16c]

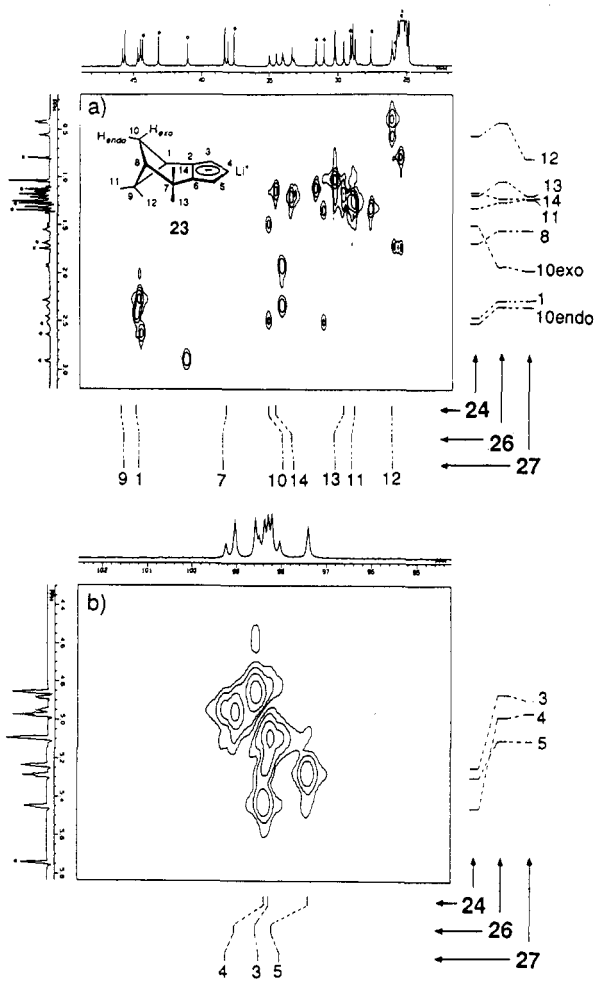

Figure 3. C,H shift-correlated 2D NMR spectrum (HETCOR) of **23** (THF-d_8, 0.35 M, −90 °C). (a) Aliphatic carbon/hydrogen atoms; (b) aromatic carbon/hydrogen atoms. The one-dimensional ^{1}H spectra are displayed with Gaussian resolution enhancement. Symbols in the one-dimensional ^{1}H spectrum are as those of Figure 1.

^{6}Li NMR Spectra. The one-dimensional ^{6}Li spectrum of **23** in THF-d_8 at −110 °C (Figure 4) is quite similar to the spectrum reported for IsodiCpLi.[4] Slightly broadened signals are observed at δ = −1.02 and δ = −7.83 ppm. We assign these signals to [Li(THF-d_8)$_4$]$^+$ (the counterion of the dimer sandwich anions in **26** and in **27**), and to Li$^+$ in monomer **24**, respectively. Whereas the ^{6}Li chemical shift

(18) Hogen-Esch, T. E. *Adv. Phys. Org. Chem.* **1977**, *15*, 153.

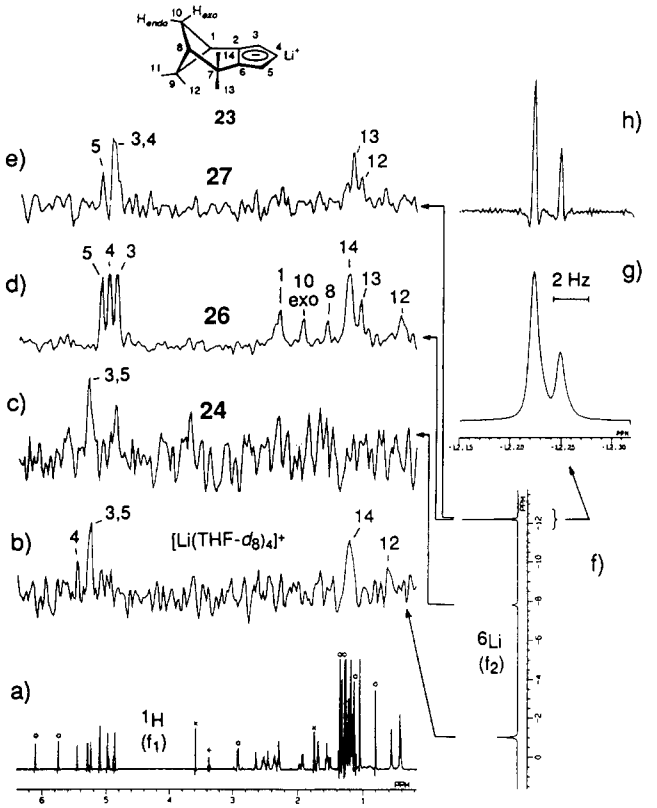

Figure 4. $^{6}Li,^{1}H$ HOESY spectrum of **23** in THF-d_8 (−110 °C, 0.65 M). Only f_1 cross sections (b–e)) cut at the chemical shifts of the four observed ^{6}Li signals (f)) are depicted. The one-dimensional ^{1}H spectrum (a) is shown with Gaussian resolution enhancement and was recorded under slightly different conditions (−90 °C, 0.35 M). The additional insets show the zoomed ^{6}Li signals at $\delta \approx -12.2$ ppm with exponential (g) and Gaussian (h) line broadening. Symbols in slice a are as those of Figure 1. For the ^{1}H chemical shift assignments, see Figure 3.

of the tetrasolvated cation is in the "normal" range of lithium chemical shifts (ca. +2, ..., −2 ppm), the strong upfield shift operating on the Li atom in **24** must be due to magnetic anisotropy. The broadness of these two signals, which persists down to −110 °C, indicates exchange between the two lithium positions to be very rapid. This is similar to our earlier observations involving IsodiCpLi[4] and CCpLi.[5]

At very high field, two resonances are detected in the ^{6}Li NMR spectrum with nearly identical chemical shifts (δ = −12.22 and −12.25 ppm; see the "zoomed" spectra in Figures 4g,4h). These signals must originate from the sandwiched lithium cations in the dimer anions **26** and **27**. The very strong upfield chemical shifts of these two resonances must be attributed to synergistic ring current effects. At a magnetic field strength of 9.4 T, the difference of the chemical shifts of these two upfield ^{6}Li resonances is only 1.5 Hz. Hence, the rate of *direct* exchange between the two lithium positions involved must be very small. The exchange between lithium positions in **24**, **26**, and **27** is likely occurring in a way very similar to the dynamics described in detail for IsodiCpLi (Scheme II in ref 4). In the present case of VCpLi (**23**), an additional "sandwich" position (termed "D" by analogy with Scheme II detailed earlier[4]) would be involved. No direct exchange between positions C and D would operate.

Figure 4 shows the $^{6}Li,^{1}H$ HOESY spectrum of **23** at −110 °C. Only f_1 cross sections cut at the four different ^{6}Li chemical shifts are depicted. In the f_1 cross section of sandwiched lithium in minor dimer **27** (Figure 4e), expected cross peaks are found that involve the Cp ring hydrogen atoms. Additional cross peaks identify the methyl groups H12 and H13. In the analogous cross section of the major dimer (Figure 4d), cross peaks involving H10(exo), H12, and H14 are observed that confirm this species to be the exo, exo dimer **26**.

Table III. Absolute Concentrations of VCpLi Monomer 24 (M) and the Sum of VCpLi Dimers 26 and 27 (D) in THF-d_8 as a Function of Temperature[a]

T (K)	$(1/T) \times 10^3$	[M] (mol/L)	[D] (mol/L)	ln K
213	4.69	0.25	0.10	0.45
203	4.93	0.20	0.12	1.09
193	5.18	0.18	0.13	1.41
183	5.46	0.14	0.16	2.05
173	5.78	0.12	0.17	2.39
163	6.13	0.09	0.19	3.15

[a] Data are obtained from integration of the individual C2 – ^{13}C NMR signals and are corrected for the density of THF at the indicated temperatures ($K = [D]/[M]^2$).

The f1 slice at the chemical shift of lithium in **24** (Figure 4c) is very noisy due to its low concentration under these conditions. Only those cross-peaks that involve the Cp ring protons are detected. For this reason, no additional hints about the location of the metal ion can be drawn from these data. However, the missing information can be retrieved from the cross section of $[Li(THF\text{-}d_8)_4]^+$ (Figure 4b). Due to the continued rapid exchange between lithium in monomer **24** and the "free" ion, $[Li(THF\text{-}d_8)_4]^+$, the NOE is mutually transferred.[15] Since the concentration of the sum of dimers **26** and **27** in Figure 4 is considerably larger than the concentration of monomer **24**, the signal-to-noise ratio in Figure 4b is higher than in Figure 4c. Clearly, cross peaks are detected in Figure 4b that involve the Cp ring protons as well as H14 of monomer **24**. A very small cross peak due to the H12 methyl protons appeared only slightly above the noise level. This is consistent with exo-positioned lithium since in the alternative isomer **25**, this cross peak would be expected to be much more intense.

Thermodynamics

The monomer–dimer equilibrium of **23** was studied by variable-temperature NMR spectroscopy. In the temperature range −110 to −70 °C, separate sets of signals were observed for the three species **24**, **26**, and **27**. In the corresponding ^{13}C NMR spectrum, only the resonances of quaternary carbon atom C2 proved to be sufficiently free of overlap for proper integration over the entire temperature range. To avoid intensity distortions by NOE, the inverse-gated decoupling technique[19] was employed. The sum of the integration values for dimers **26** and **27** was related to that of monomer **24**.

Suitable thermodynamic parameters were derived by assessing equilibrium 1 and determining the corresponding equilibrium constant K (eq 2). Here, [D] denotes the sum

$$2M \rightleftarrows D \quad (1)$$

$$K = [D]/[M]^2 \quad (2)$$

of the concentrations of dimers **26** and **27**, and [M] is the concentration of monomer **24**. M has been assessed to be a disolvated CIP, and [D] to be tetrasolvated separated solvent ion pairs (SSIPs), analogous to structures **37**, **59**, and **62** (cf. MNDO section below). Since these species are believed to prevail under the experimental conditions, the same number of solvent molecules appear on either side

(19) Friebolin, H. *Basic One- and Two-Dimensional NMR Spectroscopy*; VCH: Weinheim, FRG, 1991.

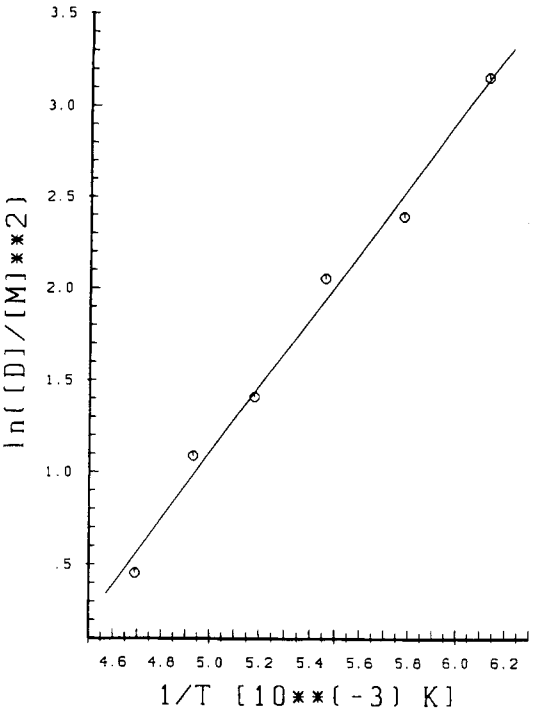

Figure 5. Van't Hoff plot (ln K vs $1/T$) of the temperature-dependent equilibrium (1) between VCpLi monomer **24** and the sum of VCpLi dimers **26** and **27**.

of eq 1 and further consideration of solvent (THF-d_8) concentration is not required.

Table III summarizes the dependence of the absolute concentrations of monomer **24** (M) and dimers **26/27** (D) on temperature. Figure 5 illustrates a van't Hoff plot derived from the data of Table III, regression analysis of which gives the thermodynamic parameters $\Delta H° = -3.6 \pm 0.2$ kcal/mol and $\Delta S° = -15.6 \pm 0.9$ eu. The negative entropy of eq 1 arises by virtue of the formation of one dimer molecule from two monomeric species. Since eq 1 is exothermic, the equilibrium shifts toward the greater levels of monomer with increasing temperature.[20] From these thermodynamic parameters, it can be extrapolated that $\Delta G_{298} = +1.1$ kcal/mol at 25 °C such that eq 1 is dominated by the left-hand side. The calculated molar ratio of [monomer] to [dimer] is 94:6. This agrees favorably with our NMR observations. From the ^1H and ^{13}C NMR chemical shifts, we have already deduced that monomer **24** must be present nearly exclusively in THF-d_8 at 26 °C.

MNDO Calculations

To help interpret the NMR investigations of **23**, semiempirical MNDO calculations[21] were carried out on a number of pertinent structures. Dimethyl ether (Me_2O) was used as a model ligand for THF since it was found to be superior to H_2O in MNDO calculations despite the increased computer demands.[22,23] Figure 6 shows various monomer (**34** to **42**) and dimer (**43** to **62**) structures of **23**, along with the calculated MNDO heats of formation

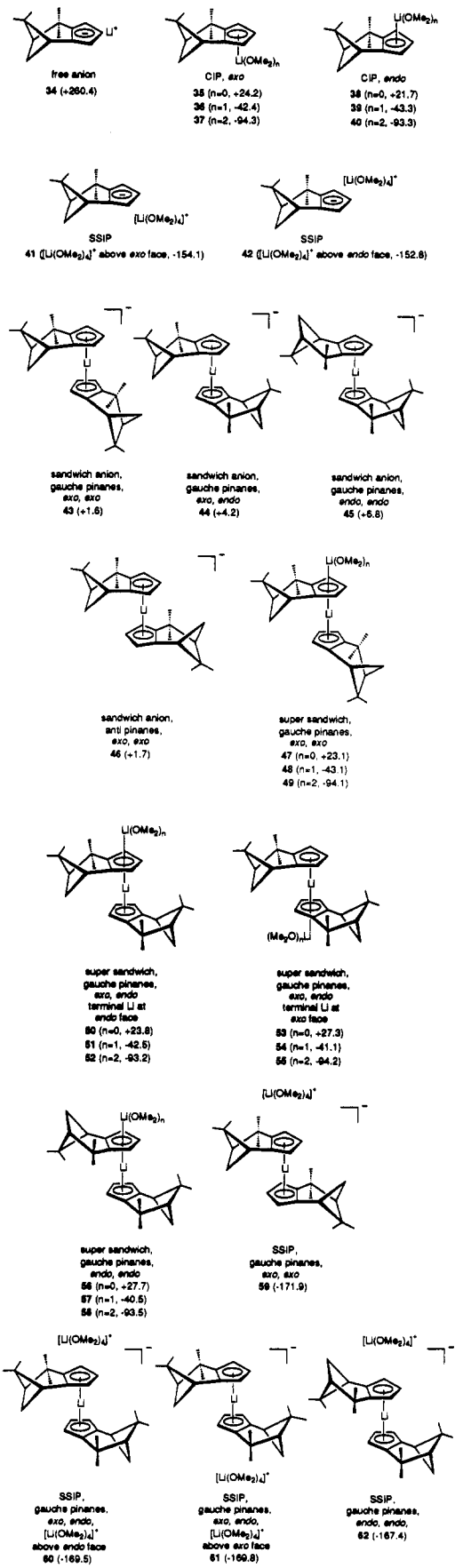

Figure 6. MNDO calculated heats of formation (kcal/mol) of various monomeric and dimeric structures of VCpLi **23**. Dimethyl ether (Me_2O) was employed as a model ligand for THF. Abbreviations: SSIP = solvent separated ion pair; CIP = contact ion pair. Additional heats of formation are: Me_2O, $\Delta H°_f = -51.2$ kcal/mol; $[Li(OMe_2)_4]^+$, $\Delta H°_f = -133.1$ kcal/mol.

(20) It is a common misconception that the *temperature dependence* of an equilibrium is governed by entropy ("the equilibrium is shifted towards the side of more particles with increasing temperature"). Rather, van't Hoff's equation clearly states that the direction of the shift of an equilibrium with temperature depends only on the sign of ΔH.

(21) Dewar, M. J. S.; Thiel, W. *J. Am. Chem. Soc.* **1977**, *99*, 4899, 4907. Li parametrization: Thiel, W.; Clark, T., unpublished.

(22) Kaufmann, E.; Gose, J.; Schleyer, P. v. R. *Organometallics* **1989**, *8*, 2577.

(23) Bauer, W.; Lochmann, L. *J. Am. Chem. Soc.* **1992**, *114*, 7482.

(kcal/mol). These structures differ in the location of lithium (exo or endo face), in the number of ligands, and in the character of the ion pair (free anions, SSIPs, and CIPs).

As reflected in eq 3, the formation of SSIP **41** from the free monomer anion **34** and $[Li(OMe_2)_4]^+$ is strongly exothermic:

$$\underset{+260.4}{\mathbf{34}} + \underset{-133.1}{[Li(OMe_2)_4]^+} \rightleftharpoons \underset{-154.1}{\mathbf{41}} \qquad \Delta H = -281.4 \text{ kcal/mol} \qquad (3)$$

Furthermore, monomeric CIP **37** is considerably more stable than the corresponding SSIP **41** (eq 4), in good

$$\underset{-154.1}{\mathbf{41}} \rightleftharpoons \underset{-94.3}{\mathbf{37}} + \underset{2 \times (-51.2)}{2Me_2O} \qquad \Delta H = -42.6 \text{ kcal/mol} \qquad (4)$$

agreement with the NMR results detailed above. In the monomeric *endo*-VCpLi **24** observed at −110 °C and at +26 °C, the lithium cation is attached tightly to the Cp ring as indicated by the upfield ^{6}Li NMR chemical shift (δ = −7.83 ppm at −110 °C) as well as by the HOESY results (Figure 4). In a hypothetical VCpLi SSIP monomer analogous to **41**, the ^{6}Li chemical shift would be near zero, and no HOESY cross peaks would be observed involving the hydrocarbon moiety.[24]

The MNDO calculations reveal nearly equal heats of formation for exo- and endo-oriented lithium in a monomeric VCpLi (eq 5). Clearly, this contrasts with the

$$\underset{-43.3}{\mathbf{39}} + \underset{-51.2}{Me_2O} \rightleftharpoons \underset{-94.3}{\mathbf{37}} \qquad \Delta H = +0.2 \text{ kcal/mol} \qquad (5)$$

experimental NMR findings. The exo isomer **24** is the only monomeric species observed at both −110 and +26 °C. We interpret this discrepancy to be a consequence of the overestimation of Li/H interactions by MNDO.[25] Such agostic[26] interactions between methyl protons H13 and Li are present in the endo isomers of **23**. The shortest computed MNDO distance, Li/H13, is 2.21 Å in monosolvate **39**. In the analogous disolvate **40**, the corresponding separation is larger by 0.21 Å. Due to these Li/H13 interactions, the corresponding C,H bond order is smaller in **39** than in **40** (0.932 vs 0.946) with greater stability accruing to **39** (eq 6).

$$\underset{-93.3}{\mathbf{40}} \rightleftharpoons \underset{-43.3}{\mathbf{39}} + \underset{-51.2}{Me_2O} \qquad \Delta H = -1.2 \text{ kcal/mol} \qquad (6)$$

Of the dimer anion sandwiches, *exo,exo*-**43** is considerably more stable than *exo,endo*-**44** and *endo,endo*-**45**. In **43**, geometry optimization started with eclipsed Cp rings and with the pinane moieties in a gauche orientation. During the optimization, a staggered pinane geometry, as shown in **43**, resulted. Interestingly, conformer **46** (having anti-pinane residues) is very slightly *less* stable than **43** (ΔH = 0.1 kcal/mol). MNDO calculations for IsodiCpLi (**1**)[4] as well as by X-ray analyses on related iron complexes gave similar results.[27]

As with the VCpLi monomer, formation of SSIP dimer **59** from the exo,exo dimer anion sandwich **43** and $[Li(OMe_2)_4]^+$ is exothermic (eq 7). The generation of **48** from

$$\underset{+1.6}{\mathbf{43}} + \underset{-133.1}{[Li(OMe_2)_4]^+} \rightleftharpoons \underset{-171.9}{\mathbf{59}} \qquad \Delta H = -37.2 \text{ kcal/mol} \qquad (7)$$

$$\underset{-171.9}{\mathbf{59}} \rightleftharpoons \underset{-43.1}{\mathbf{48}} + \underset{3 \times (-51.2)}{3Me_2O} \qquad \Delta H = -24.8 \text{ kcal/mol} \qquad (8)$$

59 follows the same pattern (eq 8), in agreement with our earlier calculations on IsodiCpLi[4] where structures analogous to **47...58** ("dimer stacks") were found to be more stable than the corresponding SSIPs (which consist of a sandwich dimer anion and $[LiL_4]^+$). Very recently, a comparable dimer stack has been observed experimentally by X-ray analysis.[28] In the so-called "super sandwich" **63**,

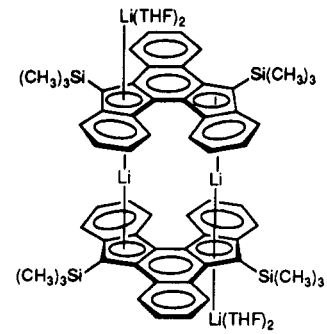

63

two different types of lithium cations are present (sandwiched unsolvated Li and external solvated Li). Note that in **63** only two THF ligands are attached to the external lithium. As previously noted,[4] disolvated species are more stable than their monosolvated analogues unless agostic methyl hydrogen/lithium interactions are involved. Calculational attempts to position three Me_2O ligands around an "external" lithium resulted in extrusion of one ligand during geometry optimization.

Of the dimer "super sandwiches" **42...58**, the exo,exo species **48** (with an external (Li × 1 Me_2O) group) is the most stable. As with the monomer (see above), the preference for only one Me_2O ligand in this isomer is presumably due to favorable interactions between lithium and the H13 methyl protons.

The MNDO result that a super sandwich (e.g., **48**) is more stable than an SSIP (e.g., **59**) contrasts with our NMR observations. Whereas for *monomeric* VCpLi the presence of a CIP is clearly indicated (see above), the two dimers **26** and **27** of VCpLi must be SSIP's. This is deduced from the ^{6}Li chemical shift of the "external" Li cation which is near zero, i.e., attributable to a $[Li(THF\text{-}d_8)_4]^+$ ion rather than to lithium in the magnetically anisotropic environment of a Cp ring. Furthermore, the ^{6}Li signals at δ = −1.02 ppm (Figure 4) shows *no* cross peaks involving the protons of the dimer sandwich moieties. This discrepancy might be a consequence of the mass effect since the presence of THF-d_8 in excess shifts the equilibrium to the side of the SSIP (cf. eq 8).

As can be seen from eq 9, the monomer–dimer equilibrium of VCpLi is exothermic (ΔH = −8.1 kcal/mol). For

$$\underset{2 \times (-94.3)}{\mathbf{237}} \rightleftharpoons \underset{-43.1}{\mathbf{48}} + \underset{3 \times (-51.2)}{3Me_2O} \qquad \Delta H = -8.1 \text{ kcal/mol} \qquad (9)$$

this reason, the equilibrium will be shifted toward the side of the *monomer* with increasing temperature (van't Hoff equation) in favorable agreement with our findings.

(24) For a related ^{6}Li, ^{1}H HOESY study on SSIPs and CIPs, see ref 16h.

(25) Kaufmann, E.; Raghavachari, K.; Reed, A. E.; Schleyer, P. v. R. *Organometallics* **1988**, *7*, 1597.

(26) (a) Brookhart, M.; Green, M. L. H. *J. Organomet. Chem.* **1983**, *250*, 395. (b) Koga, N.; Obara, S.; Morokuma, K. *J. Am. Chem. Soc.* **1984**, *106*, 4625. (c) Erker, G.; Frömberg, W.; Angermund, K.; Schlund, R.; Krüger, C. *J. Chem. Soc., Chem. Commun.* **1986**, 372.

(27) (a) Hsu, L.-Y.; Hathaway, S. J.; Paquette, L. A. *Tetrahedron Lett.* **1984**, *25*, 1597. (b) Paquette, L. A.; Schirch, P. F. T.; Hathaway, S. J.; Hsu, L.-Y.; Gallucci, J. C. *Organometallics* **1985**, *5*, 490.

(28) Malaba, D.; Chen, L.; Tessier, C. A.; Youngs, W. J. *Organometallics* **1992**, *11*, 1007.

Mechanistic Implications of Quench Reactions

The quenching of **23** with D_2O at −78 °C in THF has been shown to give **7** and **8** in a 60:40 ratio. According to NMR, **23** exists as a mixture of **24**, **26**, and **27** in 5.1:2.8:1.0 molar ratio at −80 °C (THF-d_8, c = 0.35 M). We have proposed[4] a mechanistic scheme for the electrophilic substitution at IsodiCpLi (**1**) that involves initial attachment of the negatively polarized end of the electrophile to the lithium, followed by subsequent front-side attack at the "anion" by the positively polarized terminus. The same mechanism is believed to hold for **23**. That is, during the course of a D_2O quench of **23**, the oxygen atom of the reagent is believed to attach to lithium by replacement of a solvent (THF) ligand ("front side attack"). This places the deuterium atom near the carbon where electrophile attack occurs. Whereas exo monomer **24** and endo,endo dimer **27** would lead to exo quench products, exo,exo dimer **26** would give rise to an endo product. The relevant exo/endo ratio of isomers from **23** in this instance would be predicted to be (5.1 + 2 × 1.0):(2 × 2.8) = 1.3. This value closely approaches the distribution found for the D_2O quench products (60:40 = 1.5). Hence, the molar ratio **24**:**26**:**27** manifests itself in the ratio of the quench products. Consequently, the activation energies for the D_2O quench, starting from the different lithium compounds, appear to be similar.[29] This seems reasonable with regard to the minor steric demands of the electrophile, D_2O.

By contrast, quench of the mixture of lithio compounds **24**, **26**, and **27** by the bulky electrophile, chlorotrimethylsilane, leads to strong preference of the endo over the exo product. Not surprisingly, the activation barrier leading to the exo quench product must be appreciably higher than the corresponding barrier leading to the endo diastereomer. This must be due to steric repulsion in the transition state between the sterically demanding trimethylsilyl group and the methyl group at C12.

Conclusions

The lithium salt **23** exhibits stereoselectivity in its quench reactions. When reacted with D_2O in THF solution at −78 °C, **23** yields a 60:40 endo/exo product mixture. This stereoselectivity is intrinsic to **23** as is shown by appropriate control reactions. With chlorotrimethylsilane, the preference of the endo over the exo quench product is even more pronounced. This may be ascribed to steric effects of the more bulky electrophile.

The D_2O quench results correlate with the distribution of isomers of **23** under the quench conditions determined by NMR. In THF-d_8 at −80 °C, monomer **24** and dimers **26** and **27** are present in 5.1:2.8:1.0 ratio. To our knowledge, this is only the second report of a ternary equilibrium in THF.

Identification by NMR of the various isomers of **23** was achieved by standard 2D NMR methods as well as by ^{6}Li, ^{1}H HOESY. Extrapolation of the thermodynamic data derived for the monomer–dimer equilibrium of VCpLi indicates that **23** consists nearly exclusively of exo monomer **24** at room temperature, in good agreement with the NMR observations.

According to MNDO calculations, the endo monomer **25** and the exo monomer **24** should be equally stable. This does not agree with experiment and is presumably due to the known overestimation of Li/H by the parametrization. MNDO correctly predicts the energy preference of **26** relative to **27**. Curiously, the mixed exo,endo dimer **28**, although intermediate in energy between **26** and **27**, is not detected by NMR. Finally, MNDO predicts an exothermic equilibrium between monomer **24** and the dimers **26** and **27**. Indeed, the preference of **24** at elevated temperatures is confirmed by the NMR experiments.

Experimental Section

All experiments were carried out in flame-dried glassware under an atmosphere of purified argon. n-Butyllithium enriched 96% with the ^{6}Li isotope[12] was employed for the synthesis of samples of **23** required for the NMR studies (Figures 1–4).

All solvents were reagent grade and were dried and distilled from sodium prior to use. Chlorotrimethylsilane was distilled from calcium hydride. Deuterium oxide was purchased from Aldrich and was 99.8% atom D. Chromatographic separations were performed on Kieselgel (240–400 mesh) columns or with a Waters Prep 500 LC. Melting points are uncorrected. Except for **23**, NMR spectra were obtained on a Bruker AC-300 instrument. Infrared spectra were recorded on a Perkin-Elmer 1320 spectrometer. High-resolution mass spectra were obtained at The Ohio State University Campus Chemical Instrumentation Center. Optical rotations were performed on a Perkin-Elmer 241 polarimeter using a 1-dm cell. Elemental analyses were performed at the Scandinavian Microanalytical Laboratory, Herlev, Denmark.

((1*S*,8*S*)-7,7,9,9-Tetramethyltricyclo[6.1.1.0^{2,6}]deca-2,5-dienyl)(^{6}Li)lithium (23). In a 5-mL flask was dissolved 185 mg (0.98 mmol) of **6** in 2 mL of ether. At 0 °C, 0.6 mL (1.11 mmol, 1.85 M) of n-Bu^{6}Li in hexane was added slowly with stirring. The solution was stirred at room temperature for 48 h. The white precipitate was isolated by using a D4 porosity filter stick and dried in vacuo.

(1*S*,4*R*,8*S*)-7,7,9,9-Tetramethyltricyclo[6.1.1.0^{2,6}]deca-2,5-diene-4-d_1 (7) and (1*S*,4*S*,8*S*)-7,7,9,9-Tetramethyltricyclo[6.1.1.0^{2,6}]deca-2,5-diene-4-d_1 (8). To a solution of **23** (200 mg, 1.03 mmol) in 30 mL of dry THF at −78 °C was added a solution of D_2O (90.8 mg, 4.53 mmol) in 10 mL of THF via cannula. The mixture was stirred at −78 °C for 1 h and at room temperature for 2 h, diluted with ether (50 mL), and poured into water (100 mL). The separated aqueous layer was extracted with ether (4 × 50 mL). The combined organic layers were dried, filtered, and concentrated to give a light yellow oil, which was purified on neutral alumina (elution with pentane) to give 160 mg (82%) of a 60:40 mixture of **7** and **8**; IR (neat, cm^{-1}) 2960, 2922, 2900, 2868; ^{1}H NMR (300 MHz, C_6D_6) δ 5.99 (br s, 1 H), 5.78 (t, J = 1.6 Hz, 1 H), 2.86 (br m, 1 H), 2.65 (dd, J = 5.5, 5.0 Hz, 1 H), 2.40 (ddd, J = 10, 6.5, 5.5 Hz, 1 H), 1.61 (dd, J = 6.5, 5.0 Hz, 1 H), 1.46 (d, J = 10 Hz, 1 H), 1.31 (s, 3 H), 1.26 (s, 3 H), 1.18 (s, 3 H), 0.88 (s, 3 H); ^{1}H NMR (300 MHz, CD_3COCD_3) δ 6.06 (ddd, J = 2, 1.5, 1 Hz, 1 H), 5.72 (dd, J = 2, 1.5 Hz, 1 H), 2.91 (br s, 1 H), 2.89 (br m, 1 H), 2.64 (dd, J = 5.5, 5 Hz, 1 H), 2.51 (ddd, J = 10, 6.5, 5.5 Hz, 1 H), 1.71 (dd, J = 6.5, 5 Hz, 1 H), 1.38 (d, J = 10 Hz, 1 H), 1.35 (s, 3 H), 1.29 (s, 3 H), 1.14 (s, 3 H), 0.80 (s, 3 H); ^{2}H NMR (46 MHz, CD_3COCD_3) δ 2.91 (s) and 2.82 (s); ^{13}C NMR (75 MHz, C_6D_6) ppm 153.15, 152.02, 123.87, 120.10, 54.02, 44.62, 42.73, 40.48 (t, J = 19.2 Hz), 37.17, 31.61, 30.95, 29.20, 27.73, 25.19; MS m/z (M^+) calcd for $C_{14}H_{19}D$ 189.1628, obsd 189.1631.

Deprotonation–Quench of the Deuterated Dienes 7 and 8. The product mixture from above (160 mg, 0.85 mmol) together with 30 mL of dry THF was placed in a round-bottomed flask equipped with a sidearm. The mixture was cooled to 0 °C and n-butyllithium (1.4 mL of 1.2 M, 1.69 mmol) was added via syringe. The mixture was stirred for 1 h at 0 °C before being cooled to

(29) (a) It is well recognized that the stereochemical distribution of quench products does not necessarily reflect the amount of stereoisomers of the involved organolithium compounds. As a reviewer has pointed out, "this is an error that has been made many times in organolithium chemistry". Instead, the *activation barriers* leading from the organolithium species to the quench products are of relevance for the product ratio. For a related case (the ortho lithiation of phenol), we have shown recently by ab initio calculations[29b] that the *stabilization* of the *transition state* is relevant for the ease of the reaction as compared to the lithiation of benzene. However, in the present study the distribution of the organolithium intermediates under the conditions of the quench reactions is known from NMR investigations. Hence, a comparison of the NMR determined ratio of the involved organolithium species with the quench products is legitimate and meaningful. (b) Hommes, N. J. R. v. E.; Schleyer, P. v. R. *Angew. Chem.* **1992**, *104*, 768; *Angew. Chem., Int. Ed. Engl.* **1992**, *31*, 755.

−78 °C and treated slowly after 15 min with a solution of water (76 mg, 4.23 mmol) in 20 mL of THF. The mixture was stirred at −78 °C for 1 h and at room temperature for 4 h prior to workup as before to give a light yellow oil. Analysis of the product mixture by ^2H NMR in acetone-d_6 showed the 7:8 ratio to be 45:55.

Diels–Alder Cycloaddition to 7/8. The deuterated dienes 7/8 (60:40, 190 mg, 0.98 mmol) were placed in a round-bottomed flask along with 30 mL of dry benzene, and a solution of *N*-phenylmaleimide (170 mg, 0.98 mmol) in 10 mL of benzene was introduced. The reaction mixture was stirred for 24 h at room temperature prior to concentration. The light yellow residue was purified by silica gel chromatography (elution with 20% ethyl acetate in petroleum ether) to give **9/10** (58:42) as a white solid (286 mg, 79%); IR ($CHCl_3$, cm^{-1}) 1708; ^1H NMR (300 MHz, $CDCl_3$) δ 7.42 (m, 2 H), 7.34 (m, 1 H), 7.24 (m, 2 H), 3.35 (s, 1 H), 3.18 (s, 1 H), 2.94 (d, J = 7 Hz, 1 H), 2.89 (d, J = 7 Hz, 1 H), 2.41 (ddd, J = 9, 6, 5 Hz, 1 H), 2.29 (dd, J = 5.5, 5.0 Hz, 1 H), 1.74 (dd, J = 6.0, 5.5 Hz, 1 H), 1.63 (s, 1 H), 1.48 (s, 1 H), 1.34 (s, 3 H), 1.17 (s, 3 H), 1.06 (d, J = 9 Hz, 1 H), 0.99 (s, 3 H), 0.98 (s, 3 H); ^2H NMR (46 MHz, $CDCl_3$) δ 1.80–1.30 (br m); ^{13}C NMR (75 MHz, $CDCl_3$) ppm 176.88, 176.80, 151.05, 144.16, 131.85, 128.86 (2 C), 128.24, 126.17 (2 C), 54.61, 49.20, 49.09, 48.82, 44.86, 42.95, 42.7–41.9 (m, *C*HD), 39.23, 33.57, 27.72, 27.44, 24.98, 24.04; MS m/z (M^+) calcd for $C_{24}H_{26}DNO_2$ 362.2104, obsd 362.2091.

Anal. Calcd for $C_{24}H_{26}DNO_2$: C, 79.52; H, 7.79. Found: C, 79.42; H, 7.73.

(1*S*,4*R*,8*S*)-7,7,9,9-Tetramethyl-4-(trimethylsilyl)tricyclo[6.1.1.0^{2,6}]deca-2,5-diene (11). In a 250-mL round-bottomed flask equipped with a sidearm was placed **23** (1.65 g, 8.50 mmol). To the solid was added 50 mL of dry THF, and this solution was cooled to −78 °C prior to the slow addition via cannula of chlorotrimethylsilane (1.85 g, 17.0 mmol) in 150 mL of THF at −78 °C over 20 min. The reaction mixture was allowed to stir at −78 °C for 1 h, warmed to room temperature during 2 h, poured into 500 mL of water, and extracted with ether (4 × 200 mL). The combined ethereal layers were dried, filtered, and concentrated to give a white solid as a 9:1 mixture of exo/endo isomers. The solid was purified by HPLC on silica gel (elution with petroleum ether). After several recycles to remove the minor isomer, **11** was isolated as a white solid, mp 39–41 °C (1.84 g, 83%); IR ($CHCl_3$, cm^{-1}) 2958, 2900, 2862, 1382, 1250, 875, 845; ^1H NMR (300 MHz, C_6D_6) δ 6.12 (br s, 1 H), 5.91 (dd, J = 2.0, 1.5 Hz, 1 H), 3.15 (dd, J = 1.5, 1.0 Hz, 1 H), 2.71 (dd, J = 5.5, 5.0 Hz, 1 H), 2.48 (ddd, J = 10, 6, 5.5 Hz, 1 H), 1.68 (dd, J = 6, 5 Hz, 1 H), 1.48 (d, J = 10 Hz, 1 H), 1.39 (s, 3 H), 1.31 (s, 3 H), 1.20 (s, 3 H), 0.97 (s, 3 H), −0.04 (s, 9 H); ^{13}C NMR (75 MHz, C_6D_6) ppm 151.02, 150.74, 124.77, 121.38, 54.33, 49.26, 44.70, 42.81, 37.38, 32.10, 31.94, 28.99, 27.83, 25.29, −2.0; MS m/z (M^+) calcd for $C_{17}H_{28}Si$ 260.1960, obsd 260.1972.

Diels–Alder Cycloaddition to 11. Silane **11** (73.5 mg, 0.28 mmol) was dissolved in 5 mL of benzene and 5 mL of dry hexane and then treated with *N*-phenylmaleimide (48.9 mg, 0.28 mmol) in 25 mL of benzene at room temperature. The mixture was allowed to stir at room temperature for 24 h, heated to reflux for 2 h, cooled, and concentrated to leave a yellowish solid. Silica gel chromatography (elution with 20% ethyl acetate in petroleum ether) gave an inseparable 5:1 mixture of compounds **14** and **15** (65 mg, 53%).

For **14**: ^1H NMR (300 MHz, $CDCl_3$) δ 7.50–7.35 (m, 3 H), 7.25–7.20 (m, 2 H), 3.44 (br s, 1 H), 3.30 (br s, 1 H), 3.11 (br d, J = 7 Hz, 1 H), 3.06 (br d, J = 7 Hz, 1 H), 2.45 (ddd, J = 9, 6, 5 Hz, 1 H), 2.35 (t, J = 5 Hz, 1 H), 1.73 (dd, J = 6.5 Hz, 1 H), 1.48 (d, J = 9 Hz, 1 H), 1.35 (s, 3 H), 1.17 (s, 3 H), 1.11 (s, 3 H), 1.07 (t, J = 1.5 Hz, 1 H), 0.81 (s, 3 H), −0.01 (s, 9 H).

For **15**: ^1H NMR (300 MHz, $CDCl_3$) δ 7.50–7.20 (m, 5 H), 3.44 (br s, 1 H), 3.00 (dt, J = 7.0, 1.5 Hz, 1 H), 2.91 (dd, J = 7.0, 1.5 Hz, 1 H), 2.46 (dt, J = 9, 5 Hz, 1 H), 2.39 (t, J = 5 Hz, 1 H), 1.74 (t, J = 5 Hz, 1 H), 1.61 (dq, J = 9.5, 1.5 Hz, 1 H), 1.46 (dd, J = 9.5, 1.5 Hz, 1 H), 1.37 (s, 3 H), 1.21 (s, 3 H), 1.05 (d, J = 9 Hz, 1 H), 1.03 (s, 3 H), 1.02 (s, 3 H), 0.13 (s, 9 H).

For the mixture: IR ($CHCl_3$, cm^{-1}) 1720, 1708; ^{13}C NMR (75 MHz, $CDCl_3$) ppm 177.85 (s), 177.29 (s), 177.18 (s), 176.49 (s), 153.45 (s), 151.50 (s), 145.43 (s), 142.94 (s), 132.05 (s), 129.22 (d, 2 C), 129.16 (d, 2 C), 128.80 (s), 128.60 (d), 128.50 (d), 126.41 (d, 2 C), 126.39 (d, 2 C), 54.62 (d), 54.39 (d), 51.94 (2d), 51.28 (d), 51.26 (d), 49.69 (d), 49.21 (s), 48.32 (d), 45.51 (d), 44.43 (d), 43.94 (t), 43.77 (s), 43.69 (d), 42.96 (s), 42.66 (d), 39.69 (s), 39.36 (s), 34.30 (t), 32.66 (t), 29.45 (q), 28.24 (q), 28.16 (q), 27.73 (q), 25.48 (2q), 24.46 (q), 23.66 (q), −0.47 (q, 3 C), −1.54 (q, 3 C); MS m/z (M^+) calcd for $C_{27}H_{35}NO_2Si$ 433.2437, obsd 433.2458.

Anal. Calcd for $C_{27}H_{35}NO_2Si \cdot {}^1/_2(C_2H_5)_2O$: C, 74.00; H, 8.56. Found: C, 73.99; H, 8.26.

Methylation of 23. In a 100-mL round-bottomed flask equipped with a sidearm was placed the lithium salt (200 mg, 1.03 mmol) and 25 mL of dry THF. The solution was cooled to −78 °C before methyl iodide (791 mg, 4.12 mmol) in 20 mL of THF was added via cannula. The mixture was stirred for 1 h at −78 °C and at room temperature for 1 h, diluted with ether (50 mL), and poured into water (100 mL). The separated aqueous phase was extracted with ether (3 × 100 mL), and the combined organic layers were dried, filtered, and concentrated to give a light yellow oil. NMR analysis showed that several inseparable isomers were present. This oil was directly subjected to Diels–Alder reaction.

Adduct 18. The above oil was dissolved in 30 mL of dry benzene, treated with *N*-phenylmaleimide (178 mg, 1.03 mmol), stirred at room temperature for 24 h, and concentrated. The residue was placed atop a column of silica gel and eluted with 10% ethyl acetate in petroleum ether to give **18** as the major product (112 mg, 29%); white solid, mp 59–61 °C (from petroleum ether and ethyl acetate); IR ($CHCl_3$, cm^{-1}) 1713; ^1H NMR (300 MHz, C_6D_6) δ 7.45 (m, 2 H), 7.14 (m, 2 H), 7.02 (m, 1 H), 5.58 (br s, 1 H), 2.85 (d, J = 8 Hz, 1 H), 2.68 (d, J = 11.5 Hz, 1 H), 2.55 (d, J = 8 Hz, 1 H), 2.24 (ddd, J = 11.5, 6.5, 6.0 Hz, 1 H), 1.95 (dd, J = 6, 5 Hz, 1 H), 1.92 (d, J = 8.5 Hz, 1 H), 1.51 (s, 3 H), 1.31 (dd, J = 6.5, 5.0 Hz, 1 H), 1.20 (s, 3 H), 1.08 (s, 3 H), 0.96 (s, 3 H), 0.92 (s, 3 H), 0.90 (d, J = 8.5 Hz, 1 H); ^{13}C NMR (75 MHz, $CDCl_3$) ppm 177.56 (s), 176.25 (s), 157.41 (s), 132.17 (s), 128.85 (d, 2C), 128.26 (d), 127.79 (d), 126.66 (d, 2C), 65.74 (s), 63.74 (d), 53.76 (d), 53.31 (d), 52.79 (d), 52.01 (s), 45.83 (d), 44.10 (s), 37.92 (s), 30.63 (q), 29.23 (q), 29.19 (q), 26.67 (q), 26.21 (t), 18.87 (q); MS m/z (M^+) calcd for $C_{25}H_{29}NO_2$ 375.2198, obsd 375.2183; $[\alpha]_D^{20}$ −51.9° (*c* 0.9, $CHCl_3$).

Anal. Calcd for $C_{25}H_{29}NO_2 \cdot 1/2CH_3COOC_2H_5$: C, 77.29; H, 7.93. Found: C, 77.35; H, 7.59.

Spirocyclopropanation Studies. To **23** (225 mg, 1.16 mmol) in 30 mL of dry THF at −78 °C was added 1-bromo-2-chloroethane-2,2-d_2 (337 mg, 2.32 mmol) in 10 mL of THF via cannula over 15 min. The reaction mixture was stirred for 2 h at −78 °C, at which time lithium bis(trimethylsilyl)amide (2.90 mL of 1.0 M in THF, 2.90 mmol) was introduced. Stirring was maintained at −78 °C for 1 h and at room temperature for 6 h prior to quenching with saturated NH_4Cl solution (50 mL) and extraction with ether (4 × 50 mL). The combined organic fractions were dried and concentrated to give **19** and **20** (135 mg, 54%) as a mixture of isomers; IR ($CHCl_3$, cm^{-1}) 2989, 2978, 2920, 2862; ^1H NMR (300 MHz, $CDCl_3$) δ 5.68 (br s, 1 H), 5.42 (br s, 1 H), 2.65 (dd, J = 5.5, 5.0 Hz, 1 H), 2.61 (ddd, J = 10, 6, 5.5 Hz, 1 H), 1.70 (dd, J = 6, 5 Hz, 1 H), 1.50 (d, J = 10 Hz, 1 H), 1.38 (m, 2 H), 1.36 (s, 3 H), 1.29 (s, 3 H), 1.17 (s, 3 H), 0.87 (s, 3 H); ^2H NMR (46 MHz, $CDCl_3$) 1.40 (br s); MS m/z (M^+) calcd for $C_{16}H_{20}D_2$ 216.1847, obsd 216.1871.

This mixture of **19** and **20** (130 mg, 0.60 mmol) in 50 mL of dry benzene was treated with *N*-phenylmaleimide (104 mg, 0.60 mmol) at room temperature, stirred for 24 h, and freed of solvent. Silica gel chromatography of the residue (elution with 10% ethyl acetate in petroleum ether) afforded 184 mg (84%) of **21/22** (42:58 ratio) as a colorless solid, mp 139–142 °C; IR ($CHCl_3$, cm^{-1}) 1723, 1712, 1708; ^1H NMR (300 MHz, $CDCl_3$) δ 7.45–7.20 (m, 5 H), 3.08 (d, J = 7 Hz, 1 H), 3.02 (d, J = 7 Hz, 1 H), 2.77 (s, 1 H), 2.64 (s, 1 H), 2.39 (ddd, J = 9, 6, 5 Hz, 1 H), 2.25 (dd, J = 5.5, 5.0 Hz, 1 H), 1.73 (dd, J = 6.0, 5.5 Hz, 1 H), 1.31 (s, 3 H), 1.13 (s, 3 H), 1.10 (d, J = 9 Hz, 1 H), 1.03 (s, 3 H), 0.97 (s, 3 H), for syn: 0.56 (ABq, 2 H); for anti: 0.43 (ABq, 2 H); ^2H NMR (46 MHz, $CDCl_3$) δ 0.85–0.25 (br m); ^{13}C NMR (75 MHz, $CDCl_3$) ppm 177.14, 177.06, 151.38, 144.68, 132.20, 129.10 (2 C), 128.39, 126.14 (2 C), 54.89, 54.06, 50.92, 50.14, 43.71, 42.60, 40.72, 39.47, 33.73, 27.97 (2 C), 27.71, 25.03, 23.92, 9.46, 2.79; MS m/z (M^+) calcd for $C_{26}H_{27}D_2NO_2$ 389.5376, obsd 389.2324.

Anal. Calcd for $C_{26}H_{27}D_2NO_2$: C, 80.17; H, 8.02. Found: C, 79.69; H, 7.63.

NMR Spectroscopy. NMR spectra of **23** were recorded on a JEOL GX400 spectrometer (9.4 T; ^1H, 400 MHz). ^1H and ^{13}C

NMR spectra are referenced to the signals of the deuterated solvent, THF-d_8: ^{1}H, residual α-H, δ = 3.58 ppm; ^{13}C, α-C, δ = 67.4 ppm. ^{6}Li spectra are referenced to 1M LiBr in THF/THF-d_8. The reference measurements were carried out prior to the sample measurements at the indicated temperatures. The following probe heads were employed: selective 5-mm ^{1}H (Figure 1; 90° pulse width 35 μs, attenuated), dual 5-mm ^{13}C, ^{1}H (Figure 3; 90° pulse widths 9 μs, ^{13}C, and 15 μs, ^{1}H), and 10-mm multinuclear (Figures 2 and 4; 90° pulse widths 28 μs, ^{6}Li, and 28 μs, ^{1}H). The States[30] method was employed for quadrature detection in f_1 for phase sensitive 2D NMR spectra.

Selected parameters for the individual spectra shown in the figures are as follows:

(a) Figure 1 (phase-sensitive ROESY of **23**): 0.35 M solution in THF-d_8, +26 °C, spectral width 2500 Hz (f_1 and f_2), 512 complex data points in t_2, zero filled to 1024 points, 128 t_1 increments, zero filled to 256 complex t_1 data points, 48 scans per t_1 increment, spin lock time 0.6 s (repetitive [11.7-μs pulse, 117-μs delay]$_{4668}$ sequence), Gaussian window in t_1 and t_2, interpulse delay 2.0 s.

(b) Figure 2 (phase-sensitive ^{6}Li,^{1}H HOESY of **23**): 0.35 M solution in THF-d_8, +26 °C, 5-mm sample tube, spectral widths 400 Hz (f_2, ^{6}Li) and 2500 Hz (f_1, ^{1}H), 256 complex data points in t_2, 64 increments in t_1, zero filled to 256 complex data points, 48 scans per t_1 increment, mixing time 2.0 s, Gaussian window in t_1 and t_2, interpulse delay 2.8 s.

(c) Figure 3 (magnitude mode C,H shift correlation of **23**): 0.35 M solution in THF-d_8, −90 °C, spectral widths 14970 Hz (f_2, ^{13}C) and 2500 Hz (f_1, ^{1}H), 1024 complex data points in t_2, zero filled to double size, 128 increments in t_1, zero filled to double size, 64 scans per t_1 increment, Gaussian window in t_1 and t_2 interpulse delay 2.2 s.

(d) Figure 4 (phase-sensitive ^{6}Li,^{1}H HOESY of **23**): 0.65 M solution in THF-d_8, −110 °C, spectral widths 906 Hz (f_2, ^{6}Li) and 2500 Hz (f_1, ^{1}H), 1024 complex data points in t_2, zero filled to double size, 128 increments in t_1, zero filled to double size, 32 scans per t_1 increment, mixing time 2.0 s, Gaussian window in t_1 and t_2, interpulse delay 3.0 s.

MNDO calculations were carried out on a CONVEX C220 computer by using the VAMP4 (vectorized AMPAC) program. All geometry optimizations involved the keyword EF (Eigenvector following). No symmetry constraints were imposed.

Acknowledgment. We thank T. Clark for the vectorized AMPAC program (VAMP4). Financial support by the Deutsche Forschungsgemeinschaft, the Fonds der Chemischen Industrie, the Stiftung Volkswagenwerk, the National Institutes of Health (Grant CA-12115), and the National Science Foundation is gratefully acknowledged. M.R.S. would like to thank the US Department of Education for National Need Fellowships and the Amoco Oil Company for an Amoco Foundation Fellowship.

OM920428+

(30) States, D. J.; Haberkorn, R. A.; Ruben, D. J. *J. Magn. Reson.* 1982, *48*, 286.

Synthesis of Cyclopentadienyldinitrosyl(trifluoromethyl)chromium(0), $CpCr(NO)_2CF_3$, and Cyclopentadienyldinitrosyl(trifluoromethyl)molybdenum(0), $CpMo(NO)_2CF_3$. Crystal Structure of $CpCr(NO)_2CF_3$

Demetrakis C. Loizou,[1a] Jorge Castillo,[1b] Aderemi R. Oki,[1b] Narayan S. Hosmane,*[,1b] and John A. Morrison*[,1a]

Departments of Chemistry, University of Illinois at Chicago (M/C111), Chicago, Illinois 60680, and Southern Methodist University, Dallas, Texas 75275

Received May 15, 1992

The new compounds $CpCr(NO)_2CF_3$ (71%) and $CpMo(NO)_2CF_3$ (44%) were prepared from the interactions of $Cd(CF_3)_2$·glyme (glyme = $CH_3OCH_2CH_2OCH_3$) with the chlorides at 65 °C; $CpW(NO)_2CF_3$, however, was not afforded by the analogous reaction with $CpW(NO)_2Cl$. The trifluoromethyl derivatives were characterized by ^{19}F, ^{13}C, and ^{1}H NMR, by IR, and by mass spectrometry. X-ray crystallography demonstrated that $CpCr(NO)_2CF_3$ crystallizes in the orthorhombic space group *Pnnm*, with Z = 4, a = 7.770 (4) Å, b = 10.200 (4) Å, and c = 11.179 (5) Å. The chromium complex is exceptionally thermally and oxidatively stable, but $CpMo(NO)_2CF_3$ reacts with air immediately upon exposure, and under an inert atmosphere decomposition is evident within 10 h.

Introduction

The first trifluoromethyl-containing transition-metal complexes were generated by thermal decarbonylations of CF_3CO ligands, and soon thereafter CF_3I oxidative addition was developed as the second major route to CF_3–metal derivatives. While a reasonably large number of compounds have been synthesized by these methods, each has fairly severe limitations and their utility has been largely confined to low-valent, late (electron rich) transition metals.[2]

We have been examining ligand-exchange reactions between $Cd(CF_3)_2$·glyme[3] (glyme = $CH_3OCH_2CH_2OCH_3$) and a number of main-group[4] and transition-metal halides,

(1) (a) University of Illinois at Chicago. (b) Southern Methodist University.

(2) (a) Morrison, J. A. *Adv. Inorg. Chem. Radiochem.* **1983**, *27*, 293. (b) Brothers, P. J., Roper, W. R. *Chem. Rev.* **1988**, *88*, 1293. (c) Treichel, P. M.; Stone, F. G. A. *Adv. Organomet. Chem.* **1964**, *1*, 143. (d) Morrison, J. A. *Adv. Organomet. Chem.*, submitted for publication.

(3) Krause, L. J.; Morrison, J. A. *J. Am. Chem. Soc.* **1981**, *103*, 2995. Ontiveros, C. D.; Morrison, J. A. *Inorg. Synth.* **1986**, *24*, 55.

0276-7333/92/2311-4189$03.00/0